

EFFECT OF DUST EXTINCTION ON ESTIMATING STAR FORMATION RATE OF GALAXIES:
LYMAN CONTINUUM EXTINCTIONAKIO K. INOUE, HIROYUKI HIRASHITA¹ AND HIDEYUKI KAMAYA²

Department of Astronomy, Faculty of Science, Kyoto University, Sakyo-ku, Kyoto 606-8502, JAPAN

AKI: inoue@kusastro.kyoto-u.ac.jp

accepted by ApJ

ABSTRACT

We re-examine the effect of Lyman continuum ($\lambda \leq 912 \text{ \AA}$) extinction (LCE) by dust in H II regions in detail and discuss how it affects the estimation of the global star formation rate (SFR) of galaxies. To clarify the first issue, we establish two independent methods for estimating a parameter of LCE (f), which is defined as the fraction of Lyman continuum photons contributing to hydrogen ionization in an H II region. One of those methods determines f from the set of Lyman continuum flux, electron density and metallicity. In the framework of this method, as the metallicity and/or the Lyman photon flux increase, f is found to decrease. The other method determines f from the ratio of infrared flux to Lyman continuum flux. Importantly, we show that $f \lesssim 0.5$ via both methods in many H II regions of the Galaxy. Thus, it establishes that dust in such H II regions absorbs significant amount of Lyman continuum photons directly. To examine the second issue, we approximate f to a function of only the dust-to-gas mass ratio (i.e., metallicity), assuming a parameter fit for the Galactic H II regions. We find that a characteristic \hat{f} , which is defined as f averaged over a galaxy-wide scale, is 0.3 for the nearby spiral galaxies. This relatively small \hat{f} indicates that a typical increment factor due to LCE for estimating the global SFR ($1/\hat{f}$) is large (~ 3) for the nearby spiral galaxies. Therefore, we conclude that the effect of LCE is not negligible relative to other uncertainties of estimating the SFR of galaxies.

Subject headings: dust, extinction — H II regions — galaxies: ISM — infrared: ISM: continuum — radio continuum: ISM — stars: formation

1. INTRODUCTION

When we estimate the present star formation rate (SFR) in galaxies, we use the luminosity of radiation from young massive stars as its indicator. Various observational quantities are adopted in order to count the number of photons originating from these stars. Indeed, we use the data of hydrogen recombination lines, ultraviolet (UV), infrared (IR), radio, etc., as the indicators of the photon flux and the SFR (e.g., Kennicutt 1998). Observational evidence suggests, however, that star-forming regions are often associated with dust (e.g., Glass 1999, p. 125). Thus, we cannot obtain the true SFR of galaxies unless we correct observational data for dust extinction. In other words, understanding the extinction property is important in estimating the SFR (e.g., Madau, Pozzetti, & Dickinson 1998). Therefore, we should examine the properties of dust extinction in star-forming regions in detail.

The extinction by the interstellar dust from UV ($\lambda > 912 \text{ \AA}$) to near-IR (NIR) has been studied well to date (e.g., interstellar extinction curve: Savage & Mathis 1979; Seaton 1979; Calzetti, Kinney, & Storchi-Bergmann 1994; Gordon et al. 2000). According to those researches, it is widely accepted that when we estimate the SFR from the H α luminosity, for example, we should correct decrement of the line luminosity due to the UV–NIR extinction. It can be performed by using a proper extinction curve and the observation of the Balmer decrement (e.g., Osterbrock 1989). On the other hand, how about the effect of the extinction in the Lyman continuum band? Because of the

decrement of the stellar radiation owing to the Lyman continuum extinction (LCE), we may underestimate the SFR of galaxies. In this paper, this point is extensively examined.

Indeed, many observations of H II regions have revealed that dust grains are associated with these regions (e.g., Ishida & Kawajiri 1968; Harper & Low 1971; Wynn-Williams & Becklin 1974; Frey et al. 1979; Mizuno 1982). This means a very important fact that the Lyman continuum photons from the central young massive stars suffer extinction by dust grains within H II regions. As a result, the number of Lyman continuum photons contributing to hydrogen ionization is reduced. From the intensity of recombination lines or thermal radio radiation, we can only estimate the number of the photons really contributing to the ionization. Therefore, we inevitably underestimate the number of Lyman continuum photons and the SFR unless we correct the observational data for the LCE by dust.

In studies on each individual H II region, it has been reported that a part of Lyman continuum photons are absorbed by dust if H II regions contain dust grains (e.g., Petrosian, Silk, & Field 1972; Panagia 1974; Natta & Panagia 1976; Sarazin 1977; Spitzer 1978; Mathis 1986; Aannestad 1989; Shields & Kennicutt 1995; Bottorff et al. 1998). According to Petrosian et al. (1972), for instance, the fraction of Lyman continuum photons used by hydrogen ionization is estimated to be 0.26 for the Orion nebula. Their result has shown that the chance which the Lyman continuum photons are extinguished by dust is significantly large. On

¹ Research Fellow of Japan Society for the Promotion of Science.

² Visiting Academics at Department of Physics, Oxford University, Keble Road, Oxford, OX1, 3RH, UK

a galactic scale, Smith, Biermann, & Mezger (1978) have examined LCE by dust for a large number of radio H II regions in the Galaxy, and then, have shown about half Lyman continuum photons from exciting stars in many H II regions are absorbed by dust within these regions. However, they did not discuss the effect of the LCE on estimating the SFR of galaxies.

Unfortunately, it seems that we often estimate the SFR of galaxies from Lyman continuum flux (e.g., Kennicutt 1983) without any correction of the LCE effect. Hence, it is indispensable for us to re-examine LCE by dust within H II regions and to discuss the effect of LCE on determining the SFR of galaxies. First, we formulate the way of estimating the fraction of Lyman continuum photons used by hydrogen ionization, and determine the fraction in each individual H II region of the Galaxy in section 2. We also present another way for estimating LCE by dust in section 3. Then, we discuss the effect of LCE by dust on estimating the galaxy-scale SFR in section 4. Finally, our conclusions are summarized in the last section.

2. FRACTION OF LYMAN CONTINUUM PHOTONS CONTRIBUTING TO HYDROGEN IONIZATION

The Lyman continuum photons from young massive stars in an H II region are absorbed by dust grains as well as by neutral hydrogen atoms. Then, the number of Lyman continuum photons contributing to hydrogen ionization, N'_{Ly} , is smaller than the intrinsic number of Lyman continuum photons, N_{Ly} . We parameterize this effect by f , which is defined as the fraction of Lyman continuum photons contributing to the hydrogen ionization; $N'_{\text{Ly}} = fN_{\text{Ly}}$. Unfortunately, we are able to estimate only N'_{Ly} from observations of recombination lines or thermal radio continuum. This means that the “real” SFR, which should be estimated from N_{Ly} , is $1/f$ times larger than the “apparent” SFR estimated from N'_{Ly} . Hence, if the parameter, f , is much smaller than unity, the effect of LCE by dust becomes very important to the estimation of the SFR. We call $1/f$ *correction factor* or *increment factor* for the SFR. In this section, we examine the value of f in each individual H II region in the Galaxy to find the correction factor quantitatively.

2.1. Formulation

First, when no dust grains exist in an H II region, the radius of the region is estimated to be the Strömgen radius, r_{S} . According to Spitzer (1978), we express the number of Lyman continuum photons emitted per unit time, N_{Ly} , by using the Strömgen radius, r_{S} :

$$N_{\text{Ly}} = \frac{4\pi}{3} r_{\text{S}}^3 n_{\text{e}} n_{\text{p}} \alpha^{(2)}, \quad (1)$$

where n_{e} and n_{p} are the number densities of electrons and protons, respectively, and $\alpha^{(2)}$ is the recombination coefficient excluding captures to the $n = 1$ level. Here, we employ the Case B approximation, which is the assumption that H II regions are optically thick for the photons of all Lyman-emission lines (e.g., Osterbrock 1989). We also assume spherical symmetry and spatial uniformity of H II regions in this paper for simplicity.

Next, we consider the effect of LCE by dust on the size of H II regions. The actual radius of the ionized region becomes smaller than the Strömgen radius in equation (1)

by the LCE effect. When we express the actual ionized radius as r_{i} , we obtain

$$N'_{\text{Ly}} = fN_{\text{Ly}} = \frac{4\pi}{3} r_{\text{i}}^3 n_{\text{e}} n_{\text{p}} \alpha^{(2)}. \quad (2)$$

Moreover, if the ratio of r_{i} to r_{S} is expressed by y_{i} , we obtain the following relation from equations (1) and (2),

$$f = y_{\text{i}}^3. \quad (3)$$

To estimate f , we need to find the quantitative relation between f and the amount of dust. We determine f in terms of the optical depth of dust for Lyman continuum photons. According to Hirashita et al. (2001), then, we define $\tau_{\text{S,d}}$ as the optical depth of dust for Lyman continuum photons over the Strömgen radius in order to formulate the dependence of f on the dust-to-gas ratio. Here, $\tau_{\text{S,d}}$ is approximated to be the optical depth at the Lyman limit (912 Å). When we adopt the Galactic extinction curve, the dust extinction at 912 Å is about $13E_{B-V}$ mag. Thus, $\tau_{\text{S,d}} \simeq 13E_{B-V}/2.5 \log e \simeq 12E_{B-V}$. If we assume that the dust-to-gas mass ratio, \mathcal{D} , is proportional to E_{B-V}/N_{H} , where N_{H} denotes the column number density of hydrogen, then, according to Spitzer (1978) and Hirashita et al. (2001),

$$E_{B-V} = \left(\frac{\mathcal{D}}{6 \times 10^{-3}} \right) \left(\frac{N_{\text{H}}}{5.9 \times 10^{21} \text{cm}^{-2}} \right) [\text{mag}], \quad (4)$$

where \mathcal{D} is estimated with respect to a typical Galactic value, 6×10^{-3} . Thus,

$$\tau_{\text{S,d}} = 12 \left(\frac{\mathcal{D}}{6 \times 10^{-3}} \right) \left(\frac{N_{\text{H}}}{5.9 \times 10^{21} \text{cm}^{-2}} \right). \quad (5)$$

Here, we define N_{H} as the column density over the Strömgen radius. That is, $N_{\text{H}} \equiv n_{\text{H}} r_{\text{S}}$, where n_{H} denotes the volume number density of hydrogen. Therefore, equation (5) is reduced to

$$\tau_{\text{S,d}} = 0.92 \left(\frac{\mathcal{D}}{6 \times 10^{-3}} \right) \left(\frac{n_{\text{H}}}{10^2 \text{cm}^{-3}} \right)^{1/3} \left(\frac{N_{\text{Ly}}}{10^{48} \text{s}^{-1}} \right)^{1/3}, \quad (6)$$

where r_{S} is eliminated by equation (1), and we suppose that $n_{\text{p}} \approx n_{\text{e}} \approx n_{\text{H}}$ (fully ionized in the ionized region) and that the temperature of H II regions is 10^4 K. Since we cannot observe the real number of Lyman continuum photons, N_{Ly} , we rewrite equation (6) in terms of the apparent one, $N'_{\text{Ly}} (= y_{\text{i}}^3 N_{\text{Ly}})$;

$$y_{\text{i}} \tau_{\text{S,d}} = 0.92 \left(\frac{\mathcal{D}}{6 \times 10^{-3}} \right) \left(\frac{n_{\text{H}}}{10^2 \text{cm}^{-3}} \right)^{1/3} \left(\frac{N'_{\text{Ly}}}{10^{48} \text{s}^{-1}} \right)^{1/3}. \quad (7)$$

In addition, Spitzer (1978) derived the following relation between y_{i} and $\tau_{\text{S,d}}$:

$$3 \int_0^{y_{\text{i}}} y^2 e^{y \tau_{\text{S,d}}} dy = 1, \quad (8)$$

where y is the radius normalized by r_{S} . Integrating equation (8), we obtain

$$\tau_{\text{S,d}}^3 = 3 \{ e^{\tau_{\text{d}}} (\tau_{\text{d}}^2 - 2\tau_{\text{d}} + 2) - 2 \}, \quad (9)$$

where τ_{d} is defined as $y_{\text{i}} \tau_{\text{S,d}}$. It is worthwhile to note that τ_{d} is identified with the optical depth of dust over

the actual ionized radius, r_i . According to equation (3), $f = y_i^3 = (\tau_d/\tau_{S,d})^3$. Thus, we finally obtain

$$f = \frac{\tau_d^3}{3\{e^{\tau_d}(\tau_d^2 - 2\tau_d + 2) - 2\}}. \quad (10)$$

This is the same as equation (8) in Petrosian et al. (1972).

Now, once n_H ($\approx n_e$), N'_{Ly} , and \mathcal{D} are determined, we derive $\tau_d (= y_i \tau_{S,d})$ via equation (7), and then, we calculate f by using equation (10). In Figure 1, we show the f vs. τ_d relation obtained from equation (10). Which quantity determines f the most effectively? According to figure 1, decrement of f is due to increment of the dust optical depth. Thus, to find the most effective parameter for f , let us examine the parameter dependence of the optical depth. We find in equation (7) that the optical depth increases according to the dust-to-gas ratio, Lyman continuum flux, and density of H II regions. Then, when any of those three parameters increase, f decreases. By the way, among the power indices in equation (7), that of the dust-to-gas ratio is the largest. Then, we find that f depends most largely on the dust-to-gas ratio.

One might think that the effect of helium on the ionization structure of H II regions is important (e.g., Osterbrock 1989). In H II regions, there are extremely energetic photons whose wavelengths are shorter than 504 Å. Such photons can ionize neutral helium. Hence, the number of Lyman continuum photons absorbed by hydrogen seems to decrease because of the absorption by helium. However, fortunately, almost all (96% according to Mathis 1971) photons produced by helium recombination can ionize neutral hydrogen. Therefore, we can assume safely that the number of Lyman continuum photons does not significantly decrease owing to the presence of helium. Moreover, the fraction of the photons with shorter wavelengths than 504 Å is small (0.14 in our calculation adopting the stellar spectra assumed to be the Planck function and Salpeter's IMF). Thus, the effect of helium on the photon count is small in estimating the SFR. Another effect of helium appears on the electron number density. For example, in the derivation of equation (6), we must replace $n_e = n_H$ with $n_e = n_H + n_{He}$. Since helium abundance is typically 0.1 by number, $n_e = 1.1n_H$. Hence, we consider this effect to be less significant than that caused by some other uncertainties, e.g., the change of the IMF. Therefore, we neglect these effects of helium in this paper.

2.2. Value of f for Individual H II Region in the Galaxy

Let us estimate f for the Galactic H II regions in order to estimate the effect of LCE by dust on determining the SFR. To do this, as formulated in the previous subsection, we need the data set of the number of Lyman continuum photons, the electron (or hydrogen) number density, and the dust-to-gas ratio.

The amount of dust is considered to be related to the metallicity. In this section, we determine the dust-to-gas mass ratio, \mathcal{D} , from the observational metallicity (abundance of oxygen) for each H II region, using a global relation between \mathcal{D} and (O/H) proposed and modeled by Hirashita (1999a,b).³ We display in figure 2 the global

relation between \mathcal{D} and $12 + \log(O/H)$. This is the same as Figure 4 of Hirashita et al. (2001). Here, we adopt $12 + \log(O/H) = 8.93$ as the solar abundance (Cox 2000). We should note here that this \mathcal{D} –(O/H) relation is the average relation for the interstellar medium (ISM) in nearby spirals and dwarfs. That is, we assume that \mathcal{D} –(O/H) relation of H II regions is not different significantly from the averaged \mathcal{D} –(O/H) of ISM. This assumption may not be very good, but the dust properties in H II regions are still uncertain. Hence, as a first step, we apply the \mathcal{D} –(O/H) relation of the ISM to each H II region.

We make two sets of the suitable samples to estimate f of each individual H II region. One is the sample of seven representative giant H II regions in the Galaxy. Their properties are summarized in Table 1. These H II regions are famous and have been studied well. Thus, the uncertainties of their data, especially their distance (i.e., their luminosity), can be regarded as small. Their apparent number flux of Lyman continuum photons (N'_{Ly}) are estimated from radio observations and more than about 10^{49} s^{-1} . Hereafter, we call this sample *luminous* sample. The determined f values are also shown in column (7) of Table 1. We find a good agreement between Petrosian et al.'s f and ours for the Orion nebula ($f = 0.26$). The mean f of this sample is 0.35.

The other sample is a part of H II regions observed and investigated by Caplan et al. (2000) and Deharveng et al. (2000). We select the H II regions whose kinematic distance and photometric distance are consistent within a factor of 1.5 from their sample. This is because the uncertainty in distance affects the estimation of the number of Lyman continuum photons and then prevents us from determining f reasonably. These H II regions tend to be less luminous than the sample of Table 1 and their apparent number flux of Lyman continuum photons (N'_{Ly}) are estimated from their H α luminosities. Hereafter, the sample is called to *less luminous* sample. Their properties are tabulated in Table 2. Caplan et al. (2000) also observed the Orion nebula and M16, both of which are also included in the sample in Table 1, but their H α luminosities are smaller than that expected from the radio observations adopted in Table 1. This is because Caplan et al. (2000) did not observe whole parts of these nebulae. Thus, we exclude the Orion nebula and M16 from the sample of Table 2. The finally determined f of the sample distributes over 0.5–1, and the mean is 0.8.

In Figures 3 (a)–(f), we present several relations among various parameters of our sample H II regions in Tables 1 and 2. Open symbols are H II regions in Table 1, and filled symbols are those in Table 2. In the panels of (a)–(c), we show some relations among the basic parameters to determine f . From these panels, we can check our standpoint for the subsequent considerations. Firstly, we may find, in panel (a), the sample regions with higher metallicity have larger observed Lyman continuum flux, N'_{Ly} . Indeed, the sample correlation coefficient is 0.41, so that the correlation exists with a confidence level of 95% for the sample. However, we find no correlation for the sample of Table 2 alone. We also cannot find the correlation

³ The parameters are set as $f_{in,O} = 0.1$ and $\beta_{acc} = 2\beta_{SN} = 10$. Here, $f_{in,O}$ is the dust mass fraction in the material injected from stars, and β_{acc} and β_{SN} are defined as gas consumption timescale (gas mass divided by star formation rate) normalized by dust growth timescale and by dust destruction timescale, respectively (see Hirashita 1999a for details).

for the extragalactic H II regions.⁴ Thus, we consider that the correlation in panel (a) may be caused by our sample selection. Hence, we assume it conservatively in this paper that N'_{Ly} dose not depend on the metallicity. In panel (b), the correlation between the metallicity and the electron number density, n_e , is not found. Thus, we dose not consider that n_e depends on the metallicity. In panel (c), interestingly, we can find a correlation between n_e and N'_{Ly} for only samples in Table 2.

Next, in the panels of (d)–(f), we present the dependence of f on the parameters of H II regions. The estimated f is regarded as a function of the metallicity in panel (d), i.e., as the metallicity in an H II region increases, f becomes smaller. This is because, in our formulation, the dust-to-gas ratio (i.e., metallicity) has a positive dependence on the optical depth of dust as shown in equation (7), and then, a larger dust content leads to a larger optical depth of dust and smaller f . Although the correlation in (d) is not the result directly derived via the analysis of the observational quantities, we confirm a trend that f depends on the metallicity (see also Hirashita et al. 2001). In panel (e), we also find f is related to N'_{Ly} which has a positive dependence on the dust optical depth (eq. [7]). This issue will be discussed again in section 3. We cannot find a significant correlation in panel (f), probably because n_e has a weak dependence in the dust optical depth (index 1/3 in eq. [7]) and its dynamic range is small relative to N'_{Ly} which has the same dependence in equation (7).

Now, we concentrate on the dependence of the dust-to-gas ratio (i.e., metallicity) on f , because the variation of dust-to-gas ratio has the largest influence on determining the dust optical depth as seen in equation (7). That is, we assume that the optical depth of dust is a function of the dust-to-gas ratio only. If we consider N'_{Ly} and n_e dose not depend on \mathcal{D} (or metallicity), we can re-express equation (7) as

$$\tau_d \equiv y_i \tau_{\text{S,d}} = x \left(\frac{\mathcal{D}}{6 \times 10^{-3}} \right), \quad (11)$$

where τ_d is the dust optical depth over the actual ionized radius (see section 2.1), and x is a factor containing the dependence of N'_{Ly} and $n_{\text{H}} (\approx n_e)$. We find that the best fit value of x for the adopted Galactic H II regions is 1.8, although the dispersion is large. In Figure 4, we display the estimated f of the individual H II region in our sample as a function of its dust-to-gas mass ratio, \mathcal{D} . The open and filled symbols represent the sample of Tables 1 and 2, respectively. This figure is basically identical to Figure 3 (d). The solid line is the best fit line ($x = 1.8$). We also show the lines of $x = 1.0$, and 3.0 for comparisons.

Here, let us discuss the increment factor for the SFR, $1/f$, which is introduced at the beginning of section 2. It is useful for us and readers to check quantitatively how f is affected by \mathcal{D} . As a representative case, we consider the model of $x = 2$, which corresponds with $N'_{\text{Ly}} \simeq 10^{49} \text{ s}^{-1}$ and $n_e \simeq 100 \text{ cm}^{-3}$ (nearly equal to the Lyman continuum number flux and electron number density of the Orion nebula). Numerically, from the set of equations (7) and (10), we find f to be about 0.2 for $\mathcal{D} = 6 \times 10^{-3}$ (the typical value of the ISM in the Galaxy; Spitzer 1978). If \mathcal{D} is 1/3,

1/10, or 1/100 of the Galactic value, f becomes 0.6, 0.9, or nearly unity, respectively. Thus, it is found that the increment factor for the SFR, $1/f$, increases from almost unity to about 5 as \mathcal{D} increases from 6×10^{-4} (1/10 of a typical Galactic value) to 6×10^{-3} . Clearly, the correction factor for the SFR is very sensitive to the dust-to-gas ratio (or metallicity), especially around $\mathcal{D} \sim 10^{-3}$. Hence, we should determine \mathcal{D} precisely to find an actual f and SFR. In any case, we must take account of the effect of LCE by dust at least for the objects whose metallicity is as high as that of the Orion nebula.

Smith et al. (1978) have also determined f for a numerous radio sample of giant H II regions in the Galaxy. Although our equation (7) is equivalent to their equation (A.2), there is a difference in the method of determining the dust-to-gas ratio of H II regions. Indeed, they used an empirical relation of the absorption cross section as a function of the Galactocentric radius (Churchwell et al. 1978), whereas we determine \mathcal{D} for each H II region individually as described above. The determined mean f for the giant H II regions by Smith et al. (1978) is 0.56. Since N'_{Ly} of their sample is larger than 10^{49} s^{-1} , their sample H II regions correspond to our sample in Table 1, which has mean $f = 0.35$. The estimated f values by us may be systematically small. This is due to the differences of some adopted parameters in calculation, for example, N_{H}/E_{B-V} . Also, Smith et al. (1978) took account of the effect of helium which we neglect as mentioned in the previous subsection. The parameter of f in Smith et al. is thus determined as the sum of the fractions of Lyman continuum photons absorbed by both hydrogen and helium. This increment by helium in f is about several % (up to 10%) in their framework. If the increment is removed, Smith's mean f will approach our value.

Throughout this section, we have found that the determination of \mathcal{D} is very important to estimate the “real” SFR (or f) from an observational count of Lyman continuum photons. To obtain \mathcal{D} accurately, it is a recommendable way that we use the luminosity of IR thermal emission of dust in H II regions. Since dust grains absorb the radiative energy from the young massive stars and then re-emit the energy in the IR range, the amount of dust is determined from the IR luminosity. In the next section, we discuss LCE by dust from observation of IR luminosity.

3. CORRELATION BETWEEN IR AND H α /RADIO LUMINOSITIES FOR H II REGIONS

In the previous section, we estimate the amount of dust (the dust-to-gas ratio) in H II regions from their metallicity. Since the amount of dust is also reflected in the IR emission, f is also determined from IR luminosity independently. In this section, then, we determine f by using the IR luminosity of H II regions in order to check consistency between the results of the previous and the current section.

Based on the theory of the IR emission from dust in H II regions by Petrosian et al. (1972), we formulate the relation between the observed IR luminosity, $L_{\text{IR}}^{\text{dust}}$, and the observed number of Lyman continuum photons, N'_{Ly}

⁴ We examine whether H II regions with higher metallicity have larger luminosity for the data of H II regions in M101 presented by Scowen, Dufour, & Hester (1992). The data can be taken from ADC, NASA/Goddard or CDS, Strasbourg, France via on-line.

(Inoue, Hirashita, & Kamaya 2000, 2001). The derived formula is

$$\frac{L_{\text{IR}}^{\text{dust}}(8 - 1000\mu\text{m})/L_{\odot}}{N'_{\text{Ly}}/5.63 \times 10^{43} \text{ s}^{-1}} = \frac{0.44 - 0.28f + 0.56\epsilon}{f}, \quad (12)$$

where ϵ is the average efficiency of the dust absorption for UV–optical photons from OB stars. Here, we have also adopted the Salpeter’s IMF (the stellar mass range is 0.1–100 M_{\odot}) and proper stellar properties. Moreover, the intrinsic number of Lyman continuum photons, N_{Ly} , is $5.63 \times 10^{43} \text{ s}^{-1}$ per unit solar luminosity of the bolometric luminosity of OB stars, in our calculation. As defined in the previous section, $N'_{\text{Ly}} = fN_{\text{Ly}}$. Instead of determining the SED of the IR radiation, we consider the total IR luminosity of dust, $L_{\text{IR}}^{\text{dust}}$, in the range of 8 – 1000 μm which covers almost the whole wavelength range of dust emission.

First, let us consider the correlation between the luminosities of IR and H α for H II regions. We make a cross-reference between the sample of Caplan et al. (2000) and the *IRAS* Point Source Catalog (*IRAS* PSC; Joint *IRAS* Science Working Group 1985). We select the sample H II regions by the following criteria; (a) the separation between the positions of the H α observations and sources in *IRAS* PSC is within 100". (b) $\log(F_{25}/F_{12}) \geq 0.4$. (c) $\log(F_{60}/F_{25}) \geq 0.25$. (d) $F_{100} \geq 80 \text{ Jy}$. Here, F_{12} , F_{25} , F_{60} , and F_{100} are the *IRAS* fluxes at 12, 25, 60, and 100 μm , respectively. The criterion (a) is based on the typical radius of optical H II regions ($\sim 1\text{--}10 \text{ pc}$) and *IRAS* positional error ($\lesssim 20''$, Beichman 1985). The criteria (b) – (d) are proposed by Hughes & Macleod (1989). The confidence level of the set of criteria for true association between *IRAS* sources and H II regions is more than 80% (Hughes & Macleod 1989; Codella et al. 1994). As a result, we obtain 18 H II regions (10 samples are also in Table 2) and their properties are found in Table 3.

When we suppose that the dust emission can be fitted by the modified black-body radiation of 30 K (spectral index is 1), *IRAS* 40 – 120 μm luminosity, L_{IRAS} , is $L_{\text{IRAS}}(40 - 120 \mu\text{m}) = 0.6L_{\text{IR}}^{\text{dust}}(8 - 1000 \mu\text{m})$. This correction factor is consistent with that of Calzetti et al. (2000). On the other hand, N'_{Ly} is estimated in terms of the H α luminosity corrected for interstellar extinction: $N'_{\text{Ly}}/\text{s}^{-1} = 2.83 \times 10^{45} L_{\text{H}\alpha}/L_{\odot}$, where we assume the Case B and the electron temperature of 10^4 K (Osterbrock 1989). Thus, equation (12) is reduced to

$$\frac{L_{\text{IRAS}}}{L_{\text{H}\alpha}} = \frac{F_{\text{IRAS}}}{F_{\text{H}\alpha}} = 31 \left(\frac{0.44 - 0.28f + 0.56\epsilon}{f} \right), \quad (13)$$

where F_{IRAS} and $F_{\text{H}\alpha}$ are fluxes of *IRAS* and H α , respectively. This is a theoretical relation between F_{IRAS} and $F_{\text{H}\alpha}$. Since a flux ratio does not depend on the distance to the objects, equation (13) is free from the uncertainty in the distance.

The average efficiency of dust absorption for UV–optical photons from OB stars, ϵ , is defined as $\epsilon \equiv 1 - 10^{-0.4\langle A_{\lambda} \rangle}$, where $\langle A_{\lambda} \rangle$ is an average dust absorption over the wavelength range of $\lambda = 1000 - 4000 \text{ \AA}$ in units of magnitude. This range is suitable for our purpose because the number of photons of $\lambda > 4000 \text{ \AA}$ emitted by OB stars are negligible. If we adopt the Galactic extinction curve (Savage &

Mathis 1979), then we have $\langle A_{\lambda} \rangle \simeq 7.2E(B - V)$. Thus, we obtain the following equation;

$$\epsilon = 1 - 10^{-3E(B-V)}. \quad (14)$$

Using this equation, we find $\epsilon \sim 1$ for the H II regions in Table 3.

Once we obtain the value of ϵ for each H II region from equation (14), we can determine each f from IR and H α fluxes by using equation (13). We show the estimated f in column (7) of Table 3. By definition, $f \leq 1$. However, for some sample H II regions, f appears to be greater than unity. The reason for the discrepancy will be discussed in the last paragraph of this section.

By the way, we compare the theoretical $F_{\text{IRAS}}\text{--}F_{\text{H}\alpha}$ relation with observational data on the F_{IRAS} vs. $F_{\text{H}\alpha}$ plane in Figure 5. Adopting $\epsilon = 1$, we make three lines for three values of f ; the solid, dotted, and dashed lines for $f = 1$, 0.5, and 0.1, respectively. Moreover, we make the dash-dotted line for the set of $f = 1$, $\epsilon = 0$. This corresponds to the case that only the Lyman α photons are absorbed by dust grains. As long as all Lyman α photons are absorbed by dust within H II regions and re-emitted in the IR range (Spitzer 1978; Hirashita et al. 2001), the area below the dash-dotted line on the F_{IRAS} vs. $F_{\text{H}\alpha}$ plane is the forbidden area within the framework of our theory. That is, the dash-dotted line stands for the lower boundary of *IRAS* flux corresponding to H α (Lyman continuum photon) flux in our model. While the correlation between F_{IRAS} and $F_{\text{H}\alpha}$ is expected theoretically from equation (13), we do not find a significant correlation in observational data points in figure 5 (the sample correlation coefficient is 0.35).⁵ This point is also examined in the final part of this section.

On the other hand, it is well known that there is a tight observational correlation between the IR luminosity and the number of Lyman continuum photons estimated from the radio luminosity (Wynn-Williams & Becklin 1974). Using equation (12), we compare this observational correlation with the theoretical one in figure 6. Here, we read the data directly from the figure in Wynn-Williams & Becklin (1974) and re-plotted them. The sample correlation coefficient of their data is 0.96, showing a strong correlation. The parameters of lines are the same as those in figure 5. Comparing the data and the model lines, we consider the IR luminosity of Wynn-Williams & Becklin (1974) (40 – 350 μm) is nearly equal to the whole dust-IR luminosity in equation (12) because the dust luminosity of the wavelength range of $\lambda < 40 \mu\text{m}$ or $\lambda > 350 \mu\text{m}$ is negligible (Calzetti et al. 2000). From figure 6, we find that the theoretical lines agree with the data of Wynn-Williams & Becklin (1974) excellently. This shows that our model is supported by the observation.

If we assume $\epsilon = 1$ for the sample of Wynn-Williams & Becklin (1974), we can determine their f from equation (12). We find $f = 0.45$ as an average in the current sample. Now, we compare it with another mean f value estimated by the method of the previous section. Since H II regions in figure 6 have $N'_{\text{Ly}} \gtrsim 10^{48} \text{ s}^{-1}$, we shall choose 18 regions whose N'_{Ly} is greater than 10^{48} s^{-1} from Tables 1 and 2. Thus, we obtain a mean f as being 0.56 by the method of section 2. Fortunately, we find a good agreement between the two f 's.

⁵ If the correlation coefficient is more than 0.45 for 18 samples, we can conclude that a correlation exists with a confidence level of 95%.

By the way, f values estimated by the both methods are not fully consistent with each other. For example, the sample of Wynn-Williams & Becklin (1974) includes the Orion nebula, M8, and M17 as the sample of Table 1 does. Their f values via equation (12) are 0.44, 0.59, and 0.59, respectively. Obviously, these values are larger than those of the Orion nebula, M8, and M17 in Table 1. This may be caused by the aperture difference between two photometories, IR and radio (see also the last paragraph in this section). This discrepancy may also result from our assumption in equation (12) that all of the energy of photons not used by hydrogen ionization is converted into IR radiation. Generally, the efficiency of conversion to IR radiation is never unity because of the escape of Lyman continuum photons from H II regions or the scattering of these photons by dust. As a result, we expect rather large IR luminosities for the H II regions by using equation (12).

Moreover, we cannot find in Figure 6 the trend that the more luminous H II regions have the smaller f . This trend was seen in section 2.1, where we determined f from the metallicity. This may be the effect of IR cirrus. The observed IR flux originates from dust associated with the star forming regions and from diffuse dust heated by the interstellar radiation field. If we consider that the IR surface brightness of the cirrus component is almost constant in a galaxy, the effect of cirrus contamination in the observed IR flux of an H II region is larger as its IR flux is lower. In the case, we may overestimate the IR luminosity for low luminosity regions, so that we may underestimate f of such regions.

Figure 6 has other interesting implications: First, the dash-dotted line ($f = 1$ and $\epsilon = 0$) means that only Lyman α photons heat dust grains and only this energy is re-emitted in IR. Obviously the predicted IR luminosity in this case falls short of the observed one. Next, the solid line ($f = 1$ and $\epsilon = 1$) represents the case that only the energy of photons whose wavelength is longer than the Lyman limit is absorbed by dust and re-emitted in IR. Even in this case, the predicted IR luminosity is not enough to explain the observed one. Hence, we conclude that a part of Lyman continuum photons ought to be absorbed and reprocessed by dust. The fraction of Lyman continuum photons absorbed by dust is about 0.5 or more. In terms of the fraction of the photons used by hydrogen ionization, $f \lesssim 0.5$ in many H II regions of our Galaxy. This is one of the main conclusions in the current paper.

To close this section, we must discuss a few remaining questions in the previous paragraphs: Why is f determined by our theory greater than unity for some H II regions in Table 3? Why cannot we find the observational correlation between F_{IRAS} and $F_{H\alpha}$ in figure 5? These may be because we use the *IRAS* PSC. Since the Galactic H II regions lie close to us and extend over large areas, they can never be regarded as point-like sources. Hence, the IR flux for H II regions in *IRAS* PSC may be underestimated since the aperture effect of H II regions is not neglected. Therefore, *IRAS* PSC may not be suitable when we measure the IR flux of Galactic H II regions (see also Chan & Fich 1995). Conversely, the correlation between the IR luminosity and the number of Lyman continuum photons inferred from radio observations is tight. This observational correlation is explained very well by our theory. This is be-

cause the IR luminosities of sample in Wynn-Williams & Becklin (1974) are observed in detail individually. Seeing the observational tight correlation in figure 6, the absence of the correlation in figure 5 is caused by flux underestimation of *IRAS* PSC due to the finite aperture effect. Thus, if we use the *image* data of the H II regions observed by *IRAS* or recent/future facilities such as *ISO*, *SOFIA*, *SIRTF*, or *ASTRO-F* (see Takeuchi et al. 1999 for a summary of the facilities), the observational correlation between F_{IR} and $F_{H\alpha}$ will appear.

4. EFFECT OF f ON GALACTIC SCALE

In this section, we estimate f averaged on galactic scale for the nearby spiral galaxies. Then we discuss the effect of LCE by dust on determining their galaxy-wide SFR. In the previous sections, we have discussed LCE by dust in H II regions. As shown in section 2, the parameter f strongly depends on the dust-to-gas mass ratio. For the Galactic H II regions, we show that $x \sim 2$ is appropriate in equation (11). That is, the Orion nebula is likely to be a typical Galactic H II region in gas density and Lyman continuum flux. Here, we consider the Orion nebula is also a typical H II region in the other galaxies. In short, we assume $x = 2$ in equation (11) to be universal for the galaxies. Then, we estimate a typical f for the nearby spiral galaxies from their dust-to-gas ratio. By the way, we can determine f of the galaxies from equation (13) as performed for the Galactic H II regions in section 3. This alternative way is discussed in the last part of this section.

In order to determine their dust-to-gas ratio, we estimate the amount of dust mass in the nearby spiral galaxies from their IR emission re-processed by dust. As considered in the final paragraph of section 3, we do not use *IRAS* PSC since we want to estimate the entire IR luminosity of the sample galaxies safely. We adopt only the sample galaxies whose entire images by *IRAS* are available. We note another issue here. If we convert the IR emission calculated only from *IRAS* data to the dust mass, the total amount of dust will be underestimated. This is because there is large amount of cold dust (10–20 K) in the spiral galaxies, even in those with starburst regions (Calzetti et al. 2000 and references therein). Such cold dust cannot be traced by *IRAS* bands. On the other hand, *ISO* has better detectability for the cold dust than *IRAS* because *ISO* covers longer wavelengths than *IRAS*. Thus, we expect that *ISO* data improve the estimation of dust mass.

Alton et al. (1998) present the imaging properties of seven nearby spiral galaxies obtained by both *IRAS* and *ISO*. Their sample galaxies are NGC 134, NGC 628 (M74), NGC 660, NGC 5194 (M51), NGC 5236 (M83), NGC 6946, and NGC 7331. Some basic properties of these galaxies are tabulated in tables 1, 2 and 3 of Alton et al. (1998). We estimate the dust-to-gas mass ratio for Alton's sample galaxies, and then, determine their f averaged over galactic scale. To avoid the confusion from f of the H II regions, in this section, we express the galactic f as being \bar{f} . Of course, each sample galaxy has unique \bar{f} .

We, first, calculate the dust temperature of the sample galaxies from the ratio of flux densities at 100 and 200 μm . In this calculation, we assume the spectrum of dust emission to be the modified black-body radiation with the spectral index of 1. Here, we note that the determination

of the dust temperature strongly affects the successive estimation of the dust mass. The obtained dust temperatures are shown in column (5) of Table 4. Next, we estimate the dust mass, M_d , in the sample galaxies from the observed flux density at $100 \mu\text{m}$ via the following equation:

$$M_d = \frac{4}{3} a \rho D^2 \frac{F_\nu}{Q_\nu B_\nu(T)}, \quad (15)$$

where a , ρ , and D are the grain radius, grain density, and galaxy distance, respectively. F_ν , Q_ν , and $B_\nu(T)$ are the observed flux density, grain emissivity, and the Planck function of the temperature T at the frequency ν , respectively. According to Hildebrand (1983), we set $(4/3)a\rho/Q_\nu \simeq 0.04 \text{ g cm}^{-2}$ at the frequency of $100 \mu\text{m}$ ($a = 0.1 \mu\text{m}$ and $\rho = 3 \text{ g cm}^{-3}$). The estimated dust masses are tabulated in column (6) of Table 4. Then, we determine the dust-to-gas mass ratio, \mathcal{D} , of the sample galaxies by using their total ($\text{H I} + \text{H}_2$) gas masses reported in literatures (column 7). The values of \mathcal{D} are in column (8), and the average is about 5×10^{-3} . This is quite consistent with \mathcal{D} estimated by Alton et al. (1998). Stickel et al. (2000) also claim that the median value of the dust-to-gas mass ratios of sample galaxies of ISOPHOT $170 \mu\text{m}$ Serendipity Survey (Bogun et al. 1996) is about 4×10^{-3} . Thus, our estimation of \mathcal{D} is reasonable.

It still remains open whether \mathcal{D} in H II regions can be approximated to an averaged \mathcal{D} of the ISM in the galaxies. As seen in subsection 2.2, there is a large variation of \mathcal{D} (i.e. observed metallicity) of the Galactic H II regions. Moreover, most of the sample H II regions in Tables 1 and 2 have smaller \mathcal{D} than the typical value for the Galactic ISM (6×10^{-3} ; Spitzer 1978). It may suggest that \mathcal{D} in H II regions is systematically smaller than that of the ISM. However, it is reported that the mean \mathcal{D} in the ISM is not so different from that in H II gas. Sodroski et al. (1997) have determined the dust-to-gas mass ratio of the H I, H₂, and low-density ($n_e \sim 10 \text{ cm}^{-3}$) H II gases in the Galaxy from the data of *COBE*. According to them, the mean value of \mathcal{D} in the Galactic ISM (H I + H₂ + H II) is $4.6\text{--}6.6 \times 10^{-3}$, and that in H II gas is $5.1\text{--}10 \times 10^{-3}$. With the uncertainty of a factor of 2, therefore, we assume that \mathcal{D} in H II regions is approximated to the mean \mathcal{D} of the ISM in the galaxies.

Here, let us calculate a characteristic value of the \hat{f} -parameters for the sample seven spiral galaxies, adopting their dust-to-gas mass ratio (column 8 in Table 4), equations (10) and (11) with $x = 2$. The derived values of \hat{f} are tabulated in column (9) of Table 4. The averaged \hat{f} is 0.3. This is nearly equal to the mean f of the sample H II regions in Table 1 which are more luminous than the Orion nebula. This small \hat{f} means that the correction factor of the SFR ($1/\hat{f}$; see also section 2) for these spiral galaxies is large (typically ~ 3).

Although f values of H II regions distribute over a wide range (0.02–1) as shown in Tables 1 and 2, \hat{f} is approximately equal to the averaged value of the luminous H II regions (i.e., the sample in Table 1). This may be caused by the effect of luminosity function of H II regions. Indeed, it is implied that the total luminosity of H II regions is

dominated by the regions more luminous than the Orion nebula (Kennicutt, Edgar, & Hodge 1989; Walterbos & Braun 1992; Wyder, Hodge, & Skelton 1997). Thus, \hat{f} may be shifted toward smaller values because we expect smaller f in more luminous H II regions (see section 2.1). Therefore, we think it reasonable that a characteristic \hat{f} for nearby spiral galaxies is about 0.3.

Now we discuss the importance of the increment of a factor of $1/\hat{f} \sim 3$ for the estimated SFR. There are two other major uncertainties for the estimation of the SFR. One is related to the initial mass function (IMF). The choices of a specific IMF and its upper/lower limit masses affect the coefficient of the conversion formula of the SFR. The uncertainties are within a factor of about two (e.g., Inoue et al. 2000). The other uncertainty is related to stellar properties. The choices of the stellar properties adopted affect the conversion formula of the SFR. Kennicutt, Tamblyn, & Congdon (1994) derived the formula, $\text{SFR}/M_\odot \text{ yr}^{-1} = 3.05 \times 10^{-8} L_{\text{H}\alpha}/L_\odot$, adopting their stellar population synthesis model and Salpeter IMF (0.1– $100 M_\odot$). We also derive the same type formula by using the same IMF but by using very simplified stellar properties (Inoue et al. 2001). In comparison with them, we find that the uncertainty due to the adopted stellar properties is at most a factor of two. Therefore, we conclude that the effect of LCE by dust may be more significant than the uncertainties due to the specific IMF or the stellar properties for nearby spiral galaxies.

Finally, we discuss the alternative way for determining galaxy-wide \hat{f} . We can use equation (13) to do it. However, there are three difficulties to determine \hat{f} reasonably. (i) One is the uncertainty of the cirrus fraction of the IR luminosity of the galaxies. It is widely believed that the IR luminosity of the galaxies consists of two components: the warm component originating from the dust nearby the star forming regions and the cirrus component originating from the diffuse cold dust heated by the interstellar radiation field from the older stars (e.g., Lonsdale-Persson & Helou 1987). It is a very difficult task to subtract the cirrus component from the observed IR luminosity of the galaxies in order to obtain the “pure” IR luminosity originating from the star forming regions.⁶ Since the cirrus fraction differs from galaxy to galaxy (e.g., 0.3–0.8; Lonsdale-Persson & Helou 1987), the subtraction of cirrus causes a significant uncertainty in the estimation of \hat{f} .

The other difficulties are the correction of the H α luminosity for (ii) the interstellar extinction and (iii) the [N II] contamination. Indeed, Kennicutt (1983) noted that the interstellar extinction at the wavelength of H α is 1.1 mag on average for his sample galaxies. That is, the increment correction factor for H α luminosity is 2.8. For that case, we do not neglect such large extinction in order to determine \hat{f} reasonably. At that time, we may also have to correct the inclination of the galaxies along the line of sight to find the correct \hat{f} . The [N II] contamination is more complicated if we do not have sufficient resolution of the spectrograph. Fortunately, the H α flux of Caplan et al. (2000) is not contaminated by [N II] because of their

⁶ We assumed implicitly in the previous sections that the IR emission from the H II regions is not contaminated significantly by the cirrus emission. This is because the H II regions are the star forming regions themselves. However, we may not be able to neglect the contamination of cirrus for H II regions with low luminosity.

high dispersion of spectrograph. Then, our main conclusions on f of the Galactic H II regions are not altered. However, we are sure of that the [N II] line contaminates the galactic H α emission (e.g. Kennicutt 1983). When we use equation (13) to find \hat{f} , therefore, we always need the H α luminosity corrected for the interstellar reddening and [N II] contamination to find the true \hat{f} . Unfortunately, we face the deficiency of the data to correct the H α luminosity of each individual galaxy. Because of several large uncertainties, thus, we cannot safely determine \hat{f} of the galaxies via equation (13) in this paper. This problem is examined by us in the near future.

5. CONCLUSIONS

For each individual H II region in the Galaxy, we examine LCE by dust within such regions. Then, we discuss the LCE effect on determining the SFR of galaxies. We reach the following conclusions.

[1] We estimate the fraction of Lyman continuum photons contributing to hydrogen ionization within the Galactic H II regions, f . The estimated f values distribute over a wide range (0.02–1). In our framework, an H II region with higher metallicity and larger Lyman photon flux tends to have a smaller f .

[2] From the correlation tests in Figure 3, we find that f is approximately treated as a function of only the dust-to-gas mass ratio, \mathcal{D} . For our sample of the Galactic H II regions, the Orion nebula is regarded as a typical region in gas density and Lyman continuum flux.

[3] We explain theoretically the observed correlation between IR luminosity and radio luminosity of the Galactic H II regions. Then, we manifest that a part of Lyman continuum photons (about a half or more) ought to be absorbed by dust directly in many regions.

[4] We do not find the observational correlation between fluxes of *IRAS* PSC and H α for our sample H II regions, which is expected by our model theoretically. This may indicate that *IRAS* PSC is not suitable to determine the IR flux of nearby extended sources like Galactic H II regions as pointed out in literatures.

[5] If we assume that \mathcal{D} in H II regions is not significantly different from a mean \mathcal{D} of the ISM, we estimate f averaged over galactic scale to be about 0.3 for the nearby spiral galaxies (i.e. $\hat{f} \sim 0.3$). Consequently, the increment factor for the SFR due to the LCE by dust ($1/\hat{f}$) is about 3. The correction factor is larger than the uncertainties of determining the SFR due to the choice of a specific IMF or stellar properties (within a factor of 2). Therefore, we cannot neglect the effect of LCE by dust when we estimate the SFR in galaxies.

We thank the anonymous referee for very helpful comments, which improved quality of the paper significantly. We are also grateful to Tsutomu T. Takeuchi for careful reading of this paper and giving us very useful comments. One of us (H.H.) acknowledges the Research Fellowship of the Japan Society for the Promotion of Science for Young Scientists. We have made extensive use of NASA's Astrophysics Data System Abstract Service (ADS).

REFERENCES

- Aannestad, P. A. 1989, *ApJ*, 338, 162
 Alton, P. B., Trewhella, M., Davies, J. I., Evans, R., Bianchi, S., Gear, W., Thronson, H., Valentijn, E., & Witt, A. 1998, *A&A*, 335, 807
 Beichman, C. A., Neugebauer, G., Habing, H. J., Clegg, P. E., Chester, T. J., editors 1985, *IRAS Catalogs and Atlases, Explanatory Supplement* (Washington, D.C.: U.S. GPO)
 Bogun, S., Lemke, D., Klaas, U., Herbstmeier, U., Assendorp, R et al. 1996, *A&A*, 315, L71
 Bottorff, M., LaMothe, J., Momjian, E., Verner, E., Vinković, D., & Ferland, G. 1998, *PASP*, 110, 1040
 Calzetti, D., Kinney, A. L., & Storch-Bergmann, T. 1994, *ApJ*, 429, 582
 Calzetti, D., Armus, L., Bohlin, R. C., Kinney, L., Koornneef, J., & Storch-Bergmann, T. 2000, *ApJ*, 533, 682
 Caplan, J., Deharveng, L., Peña, M., Costero, R., & Blondel, C. 2000, *MNRAS*, 311, 317
 Chan, G., & Fich, M. 1995, *AJ*, 109, 2611
 Churchwell, E., Smith, L. F., Mathis, J., Mezger, P. G., & Huchtmeier, W. 1978, *A&A*, 70, 719
 Codella, C., Felli, M., & Natale, V. 1994, *A&A*, 284, 233
 Cox, A. N. 2000, *Allen's Astrophysical Quantities 4th edition* (New York: Springer)
 Deharveng, L., Peña, M., Caplan, J., & Costero, R. 2000, *MNRAS*, 311, 329
 Devereux, N. A., & Young, J. S. 1990, *ApJ*, 359, 42
 Elfmg, T., Booth, R. S., Höglund, B., Johansson, L. E. B., & Sandqvist, Aa. 1996, *A&AS*, 115, 439
 Frey, A., Lemke, D., Thum, C., & Fahrbach, U. 1979, *A&A*, 74, 133
 Glass, I. S. 1999, *Handbook of Infrared Astronomy* (Cambridge: Cambridge University Press)
 Gordon, K. D., Clayton, G. C., Witt, A. D., & Misselt, K. A. 2000, *ApJ*, 533, 236
 Harper, D. A., & Low, F. J. 1971, *ApJ*, 165, L9
 Hildebrand, R. H. 1983, *QJRAS*, 24, 267
 Hirashita, H. 1999a, *ApJ*, 510, L99
 Hirashita, H. 1999b, *ApJ*, 522, 220
 Hirashita, H., Inoue, A. K., Kamaya, H. & Shibai, H. 2001, *A&A*, 366, 83
 Hughes, V. A., & Macleod, G. C. 1989, *AJ*, 97, 786
 Inoue, A. K., Hirashita, H., & Kamaya, H. 2000, *PASJ*, 52, 539
 Inoue, A. K., Hirashita, H., & Kamaya, H. 2001, in *The Physics of Galaxy Formation*, eds. Umemura, M., & Susa, H. (San Francisco: ASP) in press
 Ishida, K., & Kawajiri, K. 1968, *PASJ*, 20, 95
 Joint *IRAS* Science Working Group 1985, *IRAS Point Source Catalog* (Washington, DC: US GPO)
 Kennicutt, R. C. 1983, *ApJ*, 272, 54
 Kennicutt, R. C. 1984, *ApJ*, 287, 116
 Kennicutt, R. C. 1998, *ARA&A*, 36, 189
 Kennicutt, R. C., Edgar, B. K., & Hodge, P. W. 1989, *ApJ*, 337, 761
 Kennicutt, R. C., Tamblyn, P., & Congdon, C. W. 1994, *ApJ*, 435, 22
 Kennicutt, R. C., Bresolin, F., French, H., & Martin, P. 2000, *ApJ*, 537, 589
 Lonsdale-Persson, C. J., & Helou, G. 1987, *ApJ*, 314, 513
 Madau, P., Pozzetti, L., & Dickinson, M. 1998, *ApJ*, 498, 106
 Mathewson, D. S., & Ford, V. L. 1996, *ApJS*, 107, 97
 Mathis, J. S. 1971, *ApJ*, 167, 261
 Mathis, J. S. 1986, *PASP*, 98, 995
 Mezger, P. G., & Henderson, A. P. 1967, *ApJ*, 147, 471
 Mezger, P. G., Smith, L. F., & Churchwell, E. 1974, *A&A*, 32, 269
 Mizuno, S. 1982, *Ap&SS*, 87, 121
 Natta, A., & Panagia, N. 1976, *A&A*, 50, 191
 Osterbrock, D. E. 1989, *Astrophysics of Gaseous Nebulae and Active Galactic Nuclei* (Mill Valley: University Science Books)
 Panagia, N. 1974, *ApJ*, 192, 221
 Petrosian, V., Silk, J., & Field, G. B. 1972, *ApJ*, 177, L69
 Salpeter, E. E. 1955, *ApJ*, 121, 161
 Sarazin, C. L. 1977, *ApJ*, 211, 772
 Savage, B. D., & Mathis, J. S. 1979, *ARA&A*, 17, 73
 Scowen, P. A., Dufour, R. J., & Hester, J. J. 1992, *AJ*, 104, 92
 Seaton, M. J. 1979, *MNRAS*, 187, 73
 Shaver, P. A., & Goss, W. M. 1970, *Australian J. Phy. Astrophys. Suppl.*, 14, 77
 Shields, J. C., & Kennicutt, R. C. 1995, *ApJ*, 454, 807
 Smith, L. F., Biermann, P., & Mezger, P. G. 1978, *A&A*, 66, 65

- Sodroski, T. J., Odegard, N., Arendt, R. G., Dwek, E., Weiland, J. L., Hauser, M. G., & Kelsall, T. 1997, *ApJ*, 480, 173
- Spitzer, L. 1978, *Physical Processes in the Interstellar Medium* (New York: Wiley)
- Stickel, M., Lemke, D., Klaas, U., Beichman, C. A., Rowan-Robinson, M., Efstathiou, A., Bogun, S., Kessler, M. F. & Richer, G. 2000, *A&A*, 359, 865
- Takeuchi, T. T., Hirashita, H., Ohta, K., Hattori, T. G., Ishii, T. T., & Shibai, H. 1999, *PASP*, 111, 288
- Walterbos, R. A. M., & Braun, R. 1992, *A&AS*, 92, 625
- Wyder, T. K., Hodge, P. W., & Skelton, B. P. 1997, *PASP*, 109, 927
- Wynn-Williams, C. G., & Becklin, E. E. 1974, *PASP*, 86, 5

TABLE 1
REPRESENTATIVE GIANT GALACTIC H II REGIONS

Object	Distance (kpc)	N'_{Ly} (10^{48}s^{-1})	n_e (cm^{-3})	$12 + \log(\text{O}/\text{H})$	\mathcal{D} (10^{-3})	f	Reference
(1)	(2)	(3)	(4)	(5)	(6)	(7)	(8)
Orion	0.5	7.59	150	8.76	5.0	0.26	1
M8	1.1	10.6	60	8.74	4.5	0.37	1
M16	2.5	29.1	(100)	8.76	5.0	0.16	1
Rosette	1.4	43.2	13	8.20	0.79	0.85	2
M17	1.8	143	(100)	8.81	6.3	0.016	1
Carina	1.4	167	13	8.49	1.8	0.56	2
NGC3603	8.5	897	25	8.51	2.0	0.23	2

Note. — Col.(3): Number of Lyman continuum photons estimated from radio observations by using equation (2) in Mezger, Smith, & Churchwell (1974). Col.(4): Averaged electron number density from Kennicutt (1984). Two parentheses are assumed values. Col.(5): Observed Oxygen abundance from Kennicutt et al. (2000) and references therein. Col.(6): Determined dust-to-gas mass ratio by using the \mathcal{D} -(O/H) relation of figure 2 (see also Hirashita 1999a,b). Col.(7): Estimated f parameter by using equations (7), and (10).

References. — Sources of radio observations: 1. Mezger & Henderson (1967); 2. Shaver & Goss (1970)

TABLE 2
GALACTIC H II REGIONS OF CAPLAN ET AL. (2000)

Object	$L_{\text{H}\alpha}$ (10^{35} erg s $^{-1}$)	N'_{Ly} (10^{48} s $^{-1}$)	n_e (cm $^{-3}$)	$12 + \log(\text{O}/\text{H})$	\mathcal{D} (10^{-3})	f
(1)	(2)	(3)	(4)	(5)	(6)	(7)
S54	42.0	3.08	245	8.60	2.7	0.54
S88	2.17	0.16	28	8.43	1.5	0.94
S93	8.65	0.63	269	8.57	2.5	0.71
S101	3.61	0.26	7	8.34	1.1	0.97
S104	76.7	5.62	56	8.51	2.0	0.71
S127	38.4	2.81	545	8.23	0.79	0.80
S131	0.20	0.01	18	8.39	1.3	0.98
S142	16.6	1.22	21	8.27	0.89	0.94
S148	58.2	4.27	235	8.30	1.0	0.78
S153	8.90	0.65	106	8.12	0.59	0.94
S156	59.4	4.35	907	8.42	1.5	0.55
S168	18.4	1.35	137	8.30	1.0	0.87
S184	4.56	0.33	90	8.39	1.4	0.90
S206	31.8	2.33	313	8.37	1.3	0.75
S209	201	14.7	645	8.18	0.71	0.69
S211	26.0	1.91	135	8.03	0.48	0.93
S219	4.26	0.31	166	8.27	0.89	0.92
S252	5.22	0.38	144	8.35	1.2	0.89
S257	2.55	0.19	160	8.17	0.69	0.95

Note. — Col.(2): H α luminosities are calculated by $L_{\text{H}\alpha} = 4\pi D^2 F_{\text{H}\alpha}$, where D is the kinematic distance and $F_{\text{H}\alpha}$ is the H α flux corrected for interstellar extinction by Balmer decrement from Caplan et al. (2000) and the Galactic extinction properties (Savage & Mathis 1979). Col.(3): Number of Lyman continuum photons estimated from col.(2). Col.(4): Electron number density from Deharveng et al. (2000). Col.(5): Observed Oxygen abundance from Deharveng et al. (2000). Col.(6): Dust-to-gas mass ratio determined from col.(5) by using the \mathcal{D} –(O/H) relation of figure 2 (see also Hirashita 1999a,b). Col.(7): Estimated f parameter by using equations (7), and (10).

TABLE 3
 $H\alpha$ – IR CORRELATION OF THE GALACTIC H II REGIONS

Object	$E(B - V)$ (mag)	$F_{H\alpha}$ (10^{-10} erg s $^{-1}$ cm $^{-2}$)	IRAS source	F_{IRAS} (10^{-8} erg s $^{-1}$ cm $^{-2}$)	ϵ	f
(1)	(2)	(3)	(4)	(5)	(6)	(7)
S83	1.75	6.88	19223+2041	0.98	1	1.35
S93	1.76	12.6	19529+2704	6.91	1	0.49
S100	1.31	19.4	19598+3324	50.8	1	0.11
S101	0.56	6.07	19579+3509	0.22	0.98	2.49
S127	1.65	2.77	21270+5423	1.29	1	0.56
S128	1.83	6.31	21306+5540	3.53	1	0.48
S138	1.38	2.80	22308+5812	4.15	1	0.20
S146	1.57	6.16	22475+5939	4.05	1	0.42
S148	0.99	4.09	22542+5815	2.73	1	0.41
S152	1.10	9.28	22566+5830	6.68	1	0.38
S153	0.68	2.45	22571+5828	2.84	0.99	0.25
S156	1.12	16.5	23030+5958	7.34	1	0.58
S168	0.99	8.95	23504+6012	1.01	1	1.55
S206	1.36	52.1	03595+5110	2.44	1	2.32
S211	1.61	5.08	04329+5045	1.29	1	0.91
S212	0.92	13.8	04368+5021	0.73	1	2.22
S217	0.73	2.72	04551+4755	0.50	1	1.14
S252	0.33	7.90	06066+2029	3.82	0.90	0.51

Note. — Col.(2): Color excess determined from the Balmer decrement. Col.(3): $H\alpha$ fluxes corrected for interstellar extinction of col.(2) by the Galactic extinction properties (Savage & Mathis 1979). Col.(5): IRAS 40–120 μ m fluxes derived by $F_{IRAS} = 1.26 \times 10^{-11}(2.56F_{60}/Jy + F_{100}/Jy)$. Col.(6): Estimated ϵ by using equation (14). Col.(7): Estimated f by using equation (13) and col.(6).

TABLE 4
 \hat{f} OF SEVEN NEARBY SPIRAL GALAXIES

Object	Distance	F_{100}	F_{200}	T_d	$\log M_d$	$\log M_{\text{HI}+\text{H}_2}$	\mathcal{D}	\hat{f}
(1)	Mpc	(Jy)	(Jy)	(K)	(M_\odot)	(M_\odot)	(10^{-3})	(9)
	(2)	(3)	(4)	(5)	(6)	(7)	(8)	(9)
NGC 134	21.1	67.0	127	21	8.18	10.40	5.9	0.21
NGC 628	8.8	67.5	209	19	7.72	10.04	4.8	0.29
NGC 660	11.3	120	158	24	7.51	10.04	2.9	0.48
NGC 5194	6.2	303	533	22	7.62	9.88	5.5	0.24
NGC 5236	6.9	624	889	23	7.90	10.54	2.3	0.56
NGC 6946	10.1	338	743	20	8.38	10.48	8.0	0.12
NGC 7331	10.9	120	243	21	7.85	10.00	7.0	0.16

Note. — Col.(1): Object name. Col.(2): Distance from our Galaxy in Mpc from Alton et al. (1998). Cols.(3) – (4): Integrated flux density of *IRAS*-HIRES image at 100, 200 μm , respectively, from Alton et al. (1998). Col.(5): Dust temperature estimated from F_{100}/F_{200} and the modified black-body spectrum with the spectral index of 1. Col.(6): Dust mass estimated from F_{100} and T_d via equation (15). Col.(7): Total ($\text{H I} + \text{H}_2$) gas mass. The data of six galaxies except NGC 134 are taken from Devereux & Young (1990). H I and H_2 data of NGC 134 are taken from Mathewson & Ford (1996) and Elfhag et al. (1996), respectively. In the calculation of mass, the same CO– H_2 conversion factor, $X_{\text{CO}} = 2.8 \times 10^{20} [(\text{H}_2 \text{ cm}^{-2})/(\text{K km s}^{-1})]$, and the distances in col.(2) are used for all the sample galaxies. Col.(8): Dust-to-gas mass ratio. Col.(9): \hat{f} estimated \mathcal{D} and equations (10) and (11) with $x = 2$.

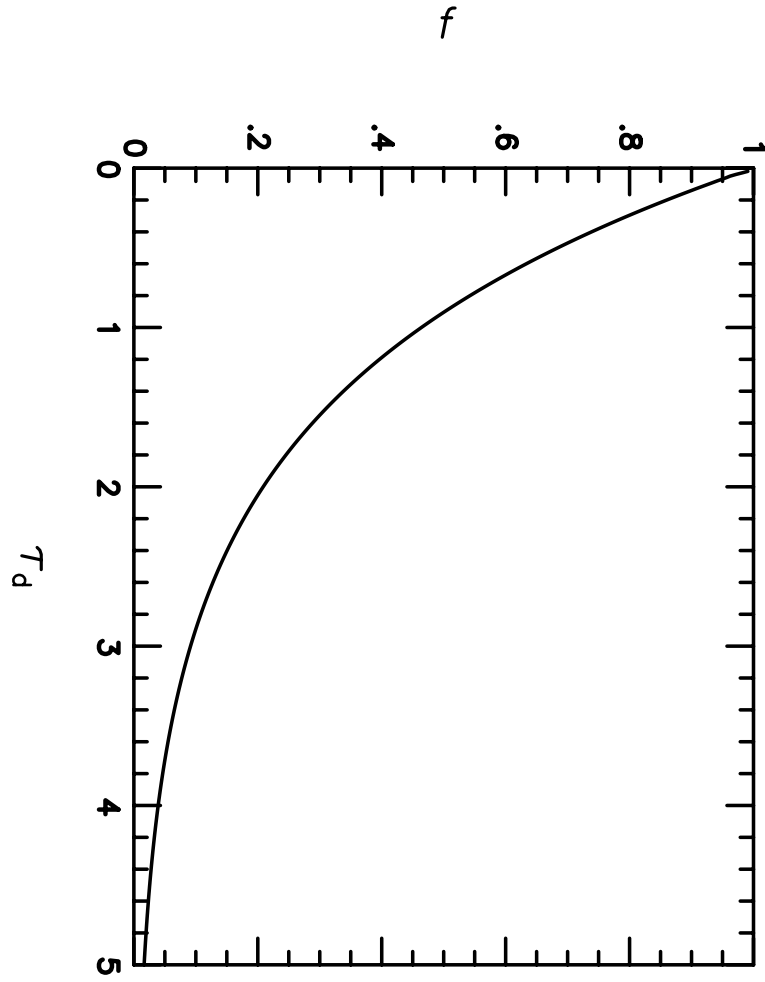


FIG. 1.— f vs. dust optical depth over actual ionized radius, τ_d .

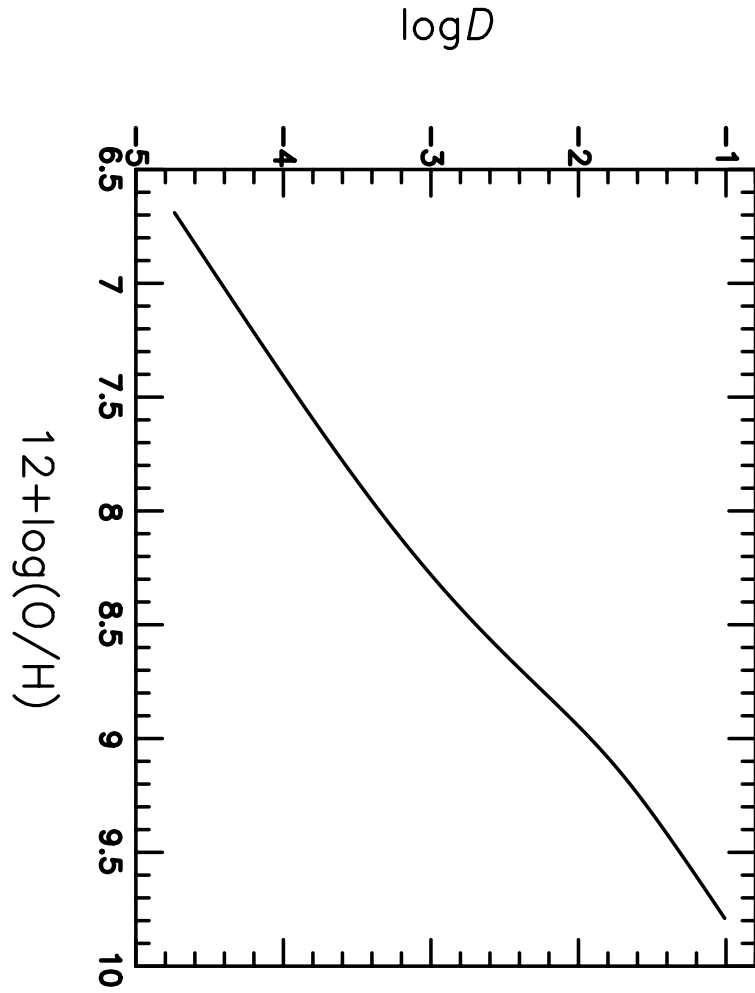


FIG. 2.— Global relation between \mathcal{D} and Oxygen abundance proposed by Hirashita (1999a,b).

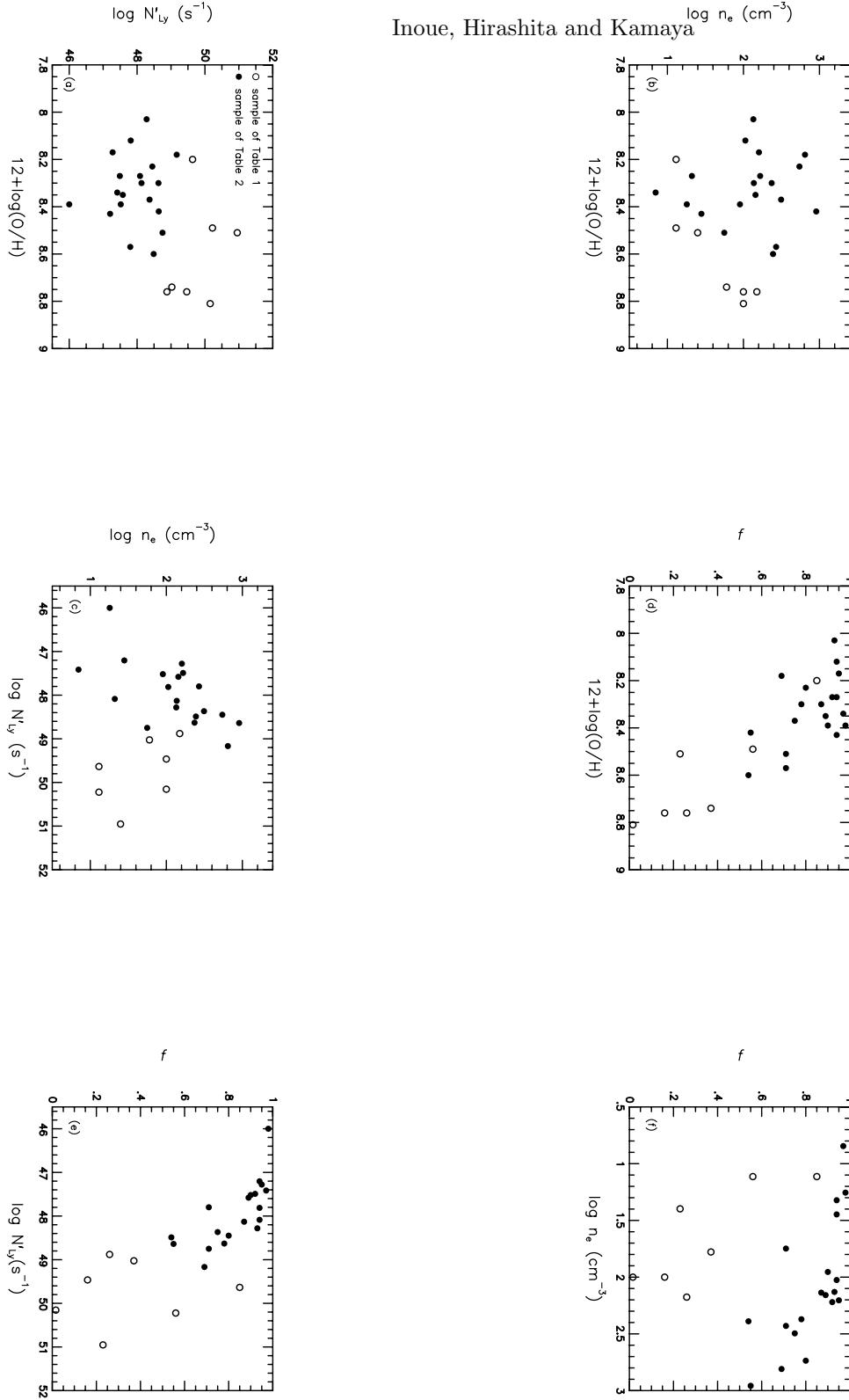


FIG. 3.— Various correlations among various properties of our sample of the Galactic H II regions. Open symbols are the samples in Table 1, and Filled symbols are the samples in Table 2. (a) metallicity vs. observed Lyman continuum number per unit time, N'_{Ly} . (b) metallicity vs. electron number density, n_e . (c) N'_{Ly} vs. n_e . (d) Estimated f vs. metallicity. (e) f vs. N'_{Ly} . (f) f vs. n_e .

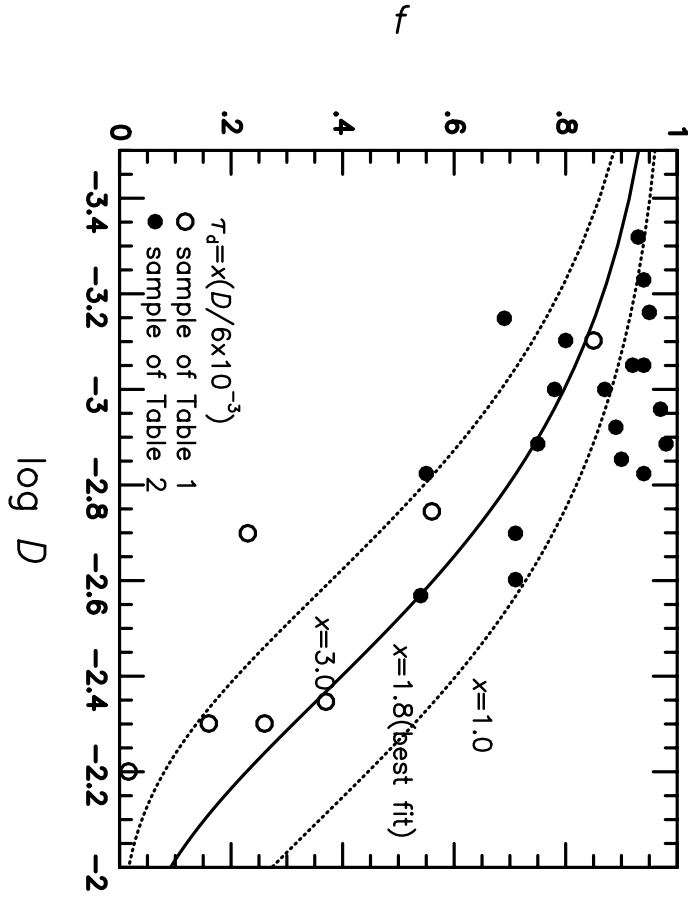


FIG. 4.— Estimated f vs. dust-to-gas mass ratio, D . Open symbols are the representative giant H II regions in Table 1, and filled symbols are H II regions in Table 2. This figure is basically the same as figure 3 (d). The solid line denotes the best fit, $x = 1.8$ in equation (11). Two dotted lines mean $x = 1.0$ and 3.0 .

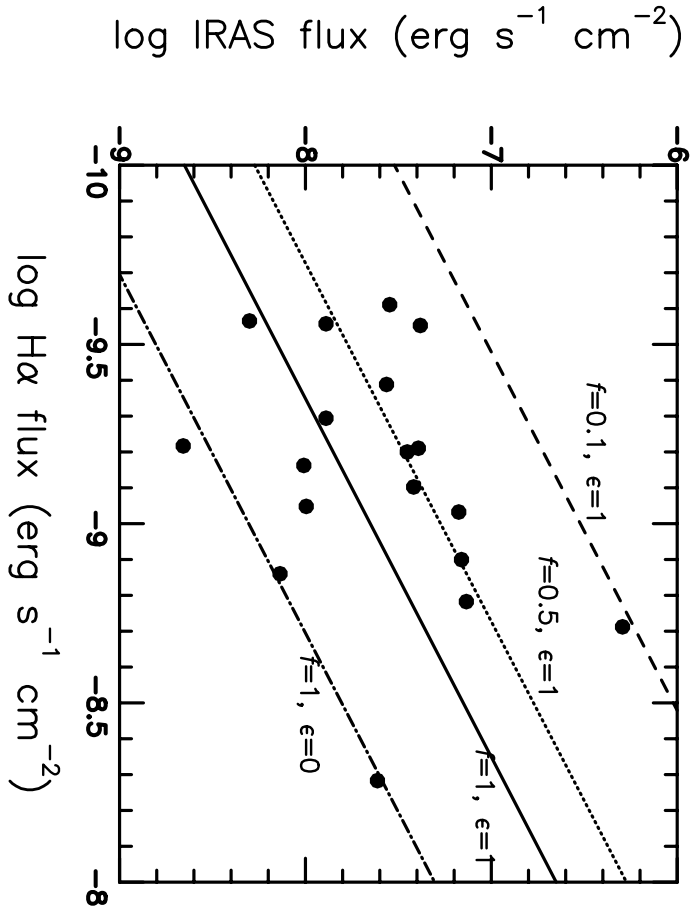


FIG. 5.— *IRAS* flux vs. $H\alpha$ flux of some Galactic H II regions. The plotted points are the sample H II regions of Table 3. The lines are the $F_{IRAS}-F_{H\alpha}$ relation expected by equation (13). The solid, dotted, and dashed lines mean $f = 1, 0.5,$ and $0.1,$ respectively, adopting $\epsilon = 1.$ We set $f = 1, \epsilon = 0$ for the dash-dotted line.

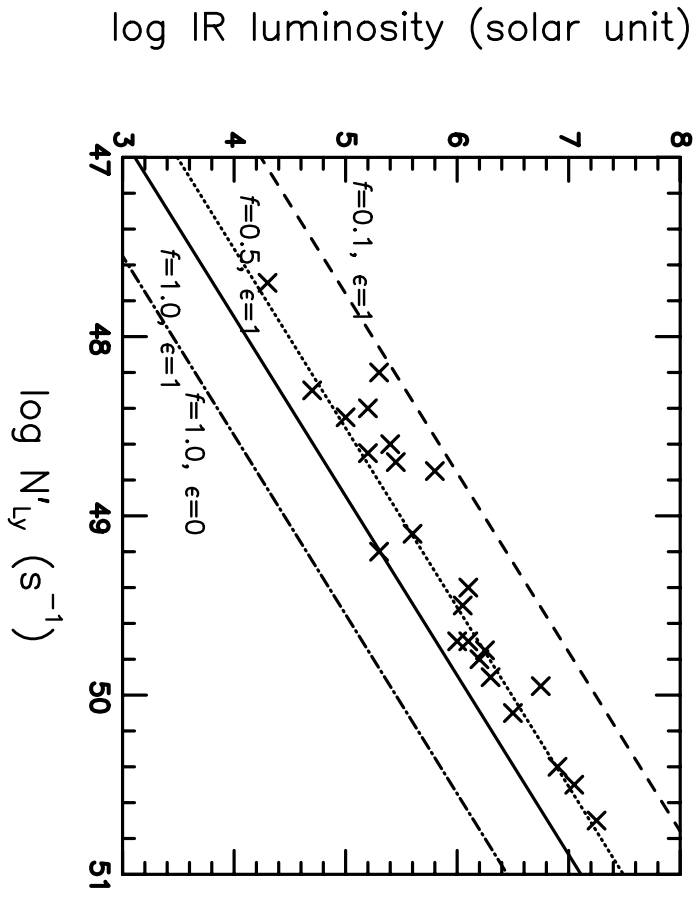


FIG. 6.— Relation between IR luminosity and number of Lyman continuum photons. The crosses are observational data for H II regions reported by Wynn-Williams & Becklin (1974). The parameter sets of lines are the same as those of figure 5.